Investigations of the Efficiency of a Detector for Heavy Ions and Feasibility Study for a New Design

A Thesis Presented to The School of Graduate Studies

Addis Ababa University

In Partial Fulfillment of the Requirement

of the Degree of Master of Science in Physics

By

Hailu Gebremariam

June 1996

Acknowledgment

I would like to express my gratefulness to my advisor Dr. K. H. Maier who has enabled me to join his research group in HMI-Berlin, Germany. I am extremely grateful for his continuous assistance, invaluable guidance and friendly encouragement without any reservation during the whole period of my work at the institute.

I extend my warmest gratitude to the member of the group, Dr. H. Grawe, Dr. K. Spohr, M. Gorska and M. Rejmund, for their encouragement and useful discussions.

It is my pleasure to express my heartfelt gratitude to my advisor and instructor Dr. S. Tesch, Addis Ababa University, for his very helpful suggestions and comments.

I wish to express my special thanks to Dr. Wendimagegn Mammo, chemistry Department, AAU, for his help in incorporating the figures.

I would like to extend my appreciation to the Deutscher Akademischer Austauschdienst (German Academic Exchange Service) DAAD- for the financial support I received during my M.Sc. study, without which the study would not have been possible.

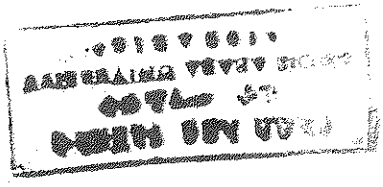

Contents

Abstract

A Recoil Filter Detector (RFD) which was developed in the Hahn-Meitner-Institut (HMI), Berlin has been investigated to determine the detector efficiency. This detector uses the forward emitted electrons from a thin mylar foil and it has been found to have lower efficiency than expected from theoretical considerations. For the test measurements a ^{252}Cf source was used. The fission products from the ^{252}Cf were detected in coincidence with the prompt γ-rays and then the spectra were analyzed. In the first part of this paper the reason for the low efficiency of the detector and the solution for an improvement is presented. In the second part, as an alternative, a new design of a detector is proposed. It uses the backward emitted electrons and may be preferred, in some aspects, to the RFD .

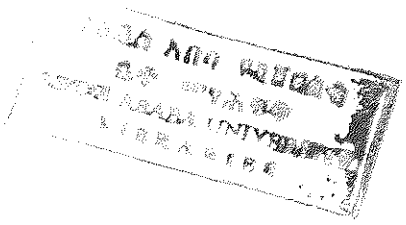

1 Introduction

A nuclear reaction is a process that occurs when a nuclear particle (nucleon or nucleus) gets into close contact with an atomic nucleus. Most of the known nuclear reactions are produced by exposing different targets to a beam of accelerated nuclear particles. Usually a large energy and momentum exchange takes place and the final products of the reaction are two or more nuclear particles leaving the point of close contact in various direction.

In general, a nuclear reaction can be expressed by the equation

$$a + X \longrightarrow Y + b \tag{1}$$

or, in more compact notation, X(a,b)Y. The notation means that particle a strikes nucleus X to produce Y and an outgoing particle b. Particles a and b may be elementary particles (neutrons, protons), but they can also themselves be nuclei (e.g. deuterons or alpha-particles).

Reaction (1) is not the most general nuclear reaction. In the general case, an arbitrary number of particles may emerge. This reaction is sufficiently general to include most of the known nuclear reactions at low energy. There is one exception to this, however, the radiative capture process, where X and a stay together to form a nucleus W while a gamma-ray is emitted:

$$a + X \longrightarrow W + \gamma \tag{2}$$

Returning to reactions of type (1), we note that formula (1) symbolizes only

one of the many possible reactions which can occur when a strikes X. The following are some of the possible reactions

$$a + X \longrightarrow \begin{cases} X + a \\ X^{*} + a \\ Y + b \\ Z + c \end{cases} \tag{3}$$

The first two reactions (3) are distinguished by the fact that the projectile a re-emerges after the reaction – elastic and inelastic scattering.

Here, attention is given to the heavy-ion fusion reaction to form a compound nucleus. In in-beam gamma-ray spectroscopy the emission of gamma-rays from the various reaction products is are studied, and from the characteristics of emitted gamma-rays, the properties of nuclear levels and the nature of highly excited states can be deduced.

Compound Nucleus. The fusion of heavy ions with nuclei offers the possibility to produce highly excited nuclei. This high excitation energy ends up partly in high thermal excitation thus making the study of "hot" compound nuclei feasible. The available energy may, however, also be converted into rotational energy. The high angular momenta involved in heavy-ion reactions will then lead to the population of very high-spin states [1]. Fusion reactions are thus an ideal tool to study the nucleus at high spin states.

In fig. 1 different reactions which can occur with heavy ions are illustrated. In the first two, complete fusion of the two nuclei to form a compound system is highly improbable, although in the second case, one or more nucleons may be transferred

or nuclear inelastic scattering may take place. In the third case, complete fusion is most likely, though some grazing orbits can induce incomplete fusion. Above the Coulomb barrier the nuclear reaction cross sections are roughly of the order of 1b for compound nucleus formation and about 5mb for single neutron transfer. Other transfer processes usually have still lower cross sections. Therefore, the dominant cross section is that for compound nucleus formation for energies not too much above the Coulomb barrier [2, 3, 4].

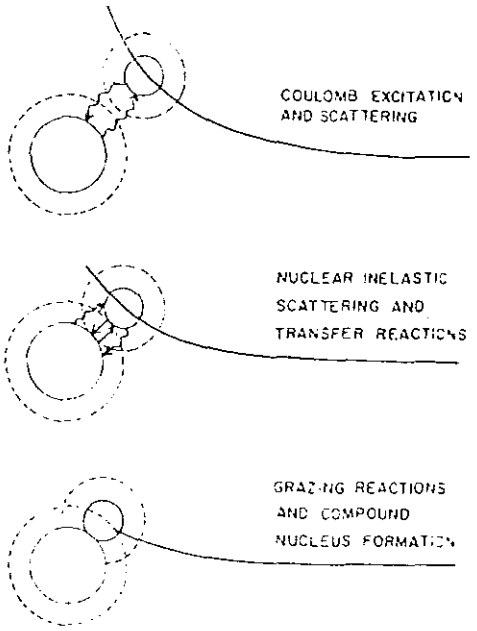

Figure 1: *Schematic illustration of different heavy-ion reactions. The large and small circles represent target and projectile, respectively. Dashed circles represent the "limits" of the tails of the nuclear wave functions. The straight arrows indicate particle transfers, and the others indicate photon transfer [5].*

High spin. One of the principal features of the heavy-ion induced reactions is the high angular momentum brought into the compound system. This aspect is of crucial importance to consider. It is now well known that there are no levels of a given angular momentum in a nucleus below some minimum energy, called the yrast energy. If a heavy ion brings in angular momentum higher than the yrast angular momentum for the appropriate excitation energy of the compound system, then a compound nucleus cannot be formed. Further, there may be some critical angular momentum for the nucleus, which, if exceeded, will result in fission. Such a critical angular momentum is quite familiar in classical physics: any rotating body will disintegrate if spun too fast. It may be independent of the excitation energy, so that even if the yrast condition for forming a compound nucleus is satisfied, the nucleus may still fly apart. Theoretical estimates of some of these phenomena have been attempted many years ago [6, 7].

After the formation of a compound nucleus fission often dominates over evaporation for heavy nuclei and very high spin [8]. The production cross section for evaporation residues may then be rather small. In these cases it is necessary to distinguish γ-rays from fusion evaporation reactions by an ancillary detector from the other strong and sometimes dominating processes. This can be accomplished by detecting evaporation residues that recoil out of the target in coincidence with the γ-rays. Recoil mass separators achieve this and in addition they determine the mass number A and sometimes the charge Z of the produced nuclei [9].

Recoil Filter Detector The low efficiency of the existing recoil mass separators, their large size and high cost makes the search for another way necessary. A considerable improvement of the interpretation of γ-spectra can be achieved when evaporation residues are detected in coincidence with γ-rays, even without exact Z and A information. This coincidence measurement suppresses γ-rays from competing fission or particle-transfer processes, Coulomb excitation or reactions with target contaminants, and therefore "cleans" γ-spectra and improves the peak to background ratio [10]. In addition, the determination of the velocity vector of the evaporation residues allows Doppler- shift corrections and therefore improves the resolution of the γ-ray energies.

Such a detector has been designed and built jointly by IFJ Krakow and HMI Berlin [11], and has been used with the OSIRIS array [12, 13] at the "VICKSI" accelerator. The comparison of the spectrum found using the RFD with the one obtained with out it, clearly indicates that there is a very good suppression of the background from accompanying reactions (fig. 2).

The OSIRIS array has a compact BGO (bismuth germanate) multielement central sphere for γ-multiplicity measurements. The average atomic number of this material is high and it is considerably denser ($7.13\ g/cm^3$) than other detector materials. So, its application is advantageous in those cases where the space is limited (for example in 4π arrays) [14]. In addition, the OSIRIS array has 12 Ge detectors with Compton suppression shields for high resolution and good detection efficiency for $\gamma\gamma$-coincidence spectroscopy.

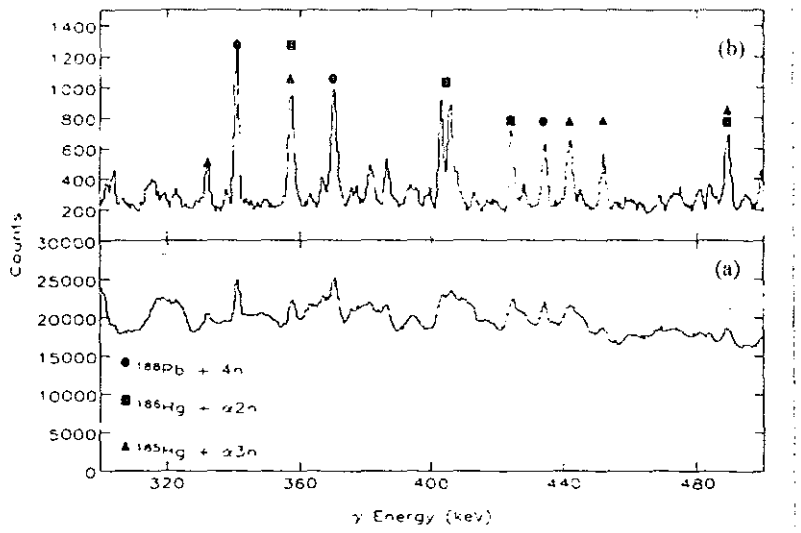

Figure 2: *In-beam measurements of $\gamma\gamma$ coincidences in the reaction $^{36}Ar + ^{156}Gd$ at 175 MeV. (a) without RFD. (b) with the RFD. Different reaction channels are indicated [10].*

A schematic diagram of the OSIRIS setup with the Recoil Filter Detector(RFD) is shown in fig. 3. The RFD consists of two rings of 6 and 12 individual detector elements (RFD-elements) mounted 73 cm from the target. At this distance time of flight separation of the heavy evaporation residues produced with not too heavy-ion beams from other reaction products is possible. The specific time structure of the recoil-gated $\gamma\gamma$ measurements is described in ref. [15].

As an example, the time of flight distribution of different reaction products is given in fig. 4 for the reaction between a beam of ^{36}Ar (E_{Kin}=173 MeV) and ^{157}Gd as a target [15]. Since most of the recoiling nuclei emerge in a narrow cone in the forward direction, the 18 detector elements are arranged in the forward direction

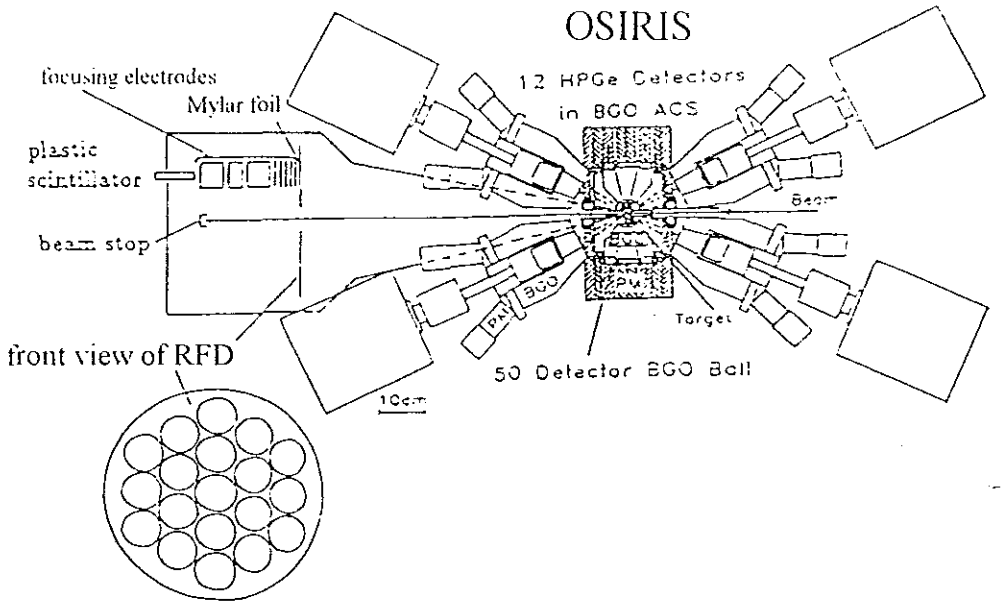

Figure 3: *Schematic diagram of the OSIRIS setup with RFD (see text)*

between 2.7^0 and 12.1^0 [10]. The central part (below 2.7^0) is left open and the direct beam passes through the open area and is stopped by a Faraday cup. In each RFD-element, nuclei hitting an aluminized mylar foil produce n secondary electrons which are electrostatically accelerated up to 20 keV and focused onto a plastic scintillator in which they produce a signal of energy approximately equal to n×20 keV. Electron yields of n≈ 100/ion are expected for slow and heavy evaporation residues [15]. Signals from scattered beam particles are suppressed by selecting only RFD signals in a time window appropriate for evaporation residues relative to the pulsed beam (fig. 4). In a second stage a $\gamma\gamma$−RFD coincidence is required. The time of flight of the heavy evaporation residues with respect to the radio frequency of the cyclotron is measured and the responding detector element is identified that

determines the recoil angle. The distance where each detector element is located is known. Therefore, using these parameters (the time of flight, the distance and the recoil angle) the velocity vector of the residues can be determined to correct the energies due to the Doppler shift of the γ-rays. This results in a good accuracy in determining the γ-energy.

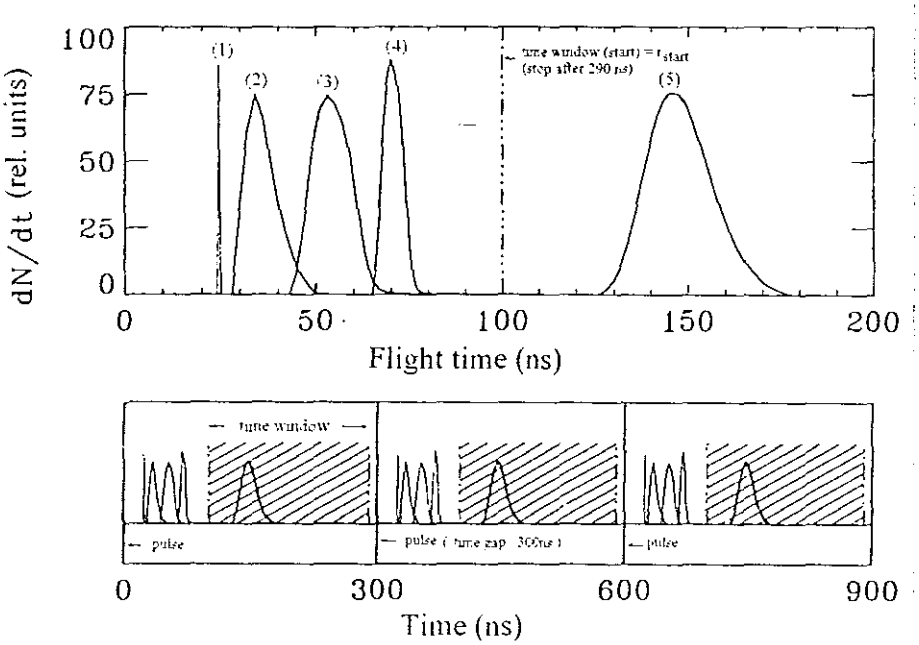

Figure 4: *Time of flight distribution of different reaction products for a beam of* ^{36}Ar *with* E_{kin}*=173 MeV and* ^{157}Gd *target. (1)- beam particles, (2)-* ^{16}O *reaction product, (3)- fission product, (4)- Coulomb excitation and (5)- evaporation resdidues [15].*

Different experiments [12, 13, 16] were done using the RFD, and in all experiments only about half of the efficiency expected from theoretical calculations [15] was achieved . Despite the fact that the detection efficiency was found to be only

12%, the requirement of recoil-γ coincidence effectively cleans the spectra from unwanted background and improves the energy resolution (see fig. 2) if Doppler shift correction is carried out.

The purpose of this work was to find out why the efficiency of the detector (RFD) is not as expected from theoretical considerations. In addition, if possible, one should get a solution for improvement. The experiments presented are aimed at looking for the reason of low RFD efficiency and the results are presented in the following sections to explain how one can increase the efficiency.

In the second part of this paper, it is dealt with a design of a detector which has the same purpose as the RFD but a different detection principle. That is, instead of using the forward emitted electrons (as it is done with the RFD), the electrons coming out in the backward direction will be used by the newly designed detector. Some experimental results will be shown supporting the new detector design.

2 Tests with the Recoil Filter Detector

The Recoil Filter Detector (RFD) consists of 18 elements of which one is used in the test experiment. The schematic diagram of the cross section of the RFD element is shown on fig. 5. The electron trajectories are calculated using the program SIMION [17]. The element has cylindrical symmetry consisting of several electrodes of different size and shape. The first electrode is connected to a negative high voltage distributed among the other electrodes by a voltage divider.

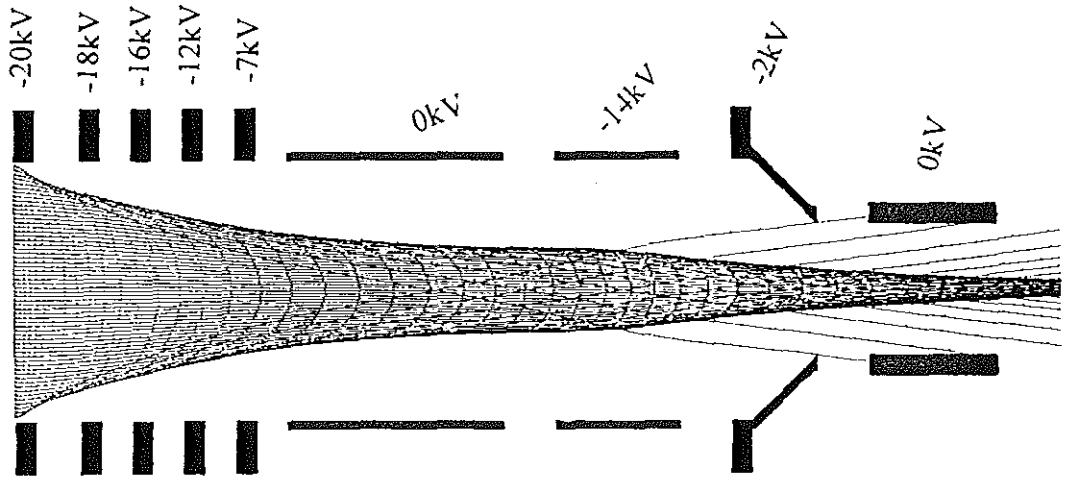

Figure 5: *The Recoil-Filter Detector-element used in the experiment with the trajectories of electrons for the accelerating voltage of* -20 *kV.*

The principle of detection of heavy ions is as follows :

A particular nucleus hitting the thin aluminized mylar foil mounted on the first electrode liberates electrons, and they are emitted in all directions [18]. The forward

emitted electrons are accelerated by the electric field present inside the element. In addition, they are focused since the element has this particular geometrical arrangement and the appropriate division of the high voltage. A fast plastic scintillator is placed in the focal plane of the detector. Each electron bunch produces a signal in the photomultiplier (PM) tube. The output signal from the PM is fed to the appropriate electronics.

In the experiment, a californium (^{252}Cf) source is used (see fig. 6). The source produces heavy nuclei which are to be detected in the way described above. This allows to simulate the in-beam nuclear reaction and to detect the fission products instead of the evaporation residues from the heavy-ion reaction.

The californium isotope ^{252}Cf decays in two modes [19], one is alpha decay (96.9%) and the other is spontaneous fission (3.1%). The main aim of the test experiment is to measure the heavy fission products. In principle, one can select the heavy fission products out of the large amount of α's by measuring them in coincidence with the prompt γ-rays. However, the alpha particles are important as well. Since they have an energy of about 6MeV, without any major effect on their kinetic energy they will pass through the thin mylar foil (thickness 0.5μm) and directly fall on the scintillator. The plastic scintillator, on the other hand, is thick enough so that it can stop and detect these energetic alpha particles.

The α-particles are detected independent of the voltage divider and the particular geometry of the electrodes of the detector element. This allows to check if the other

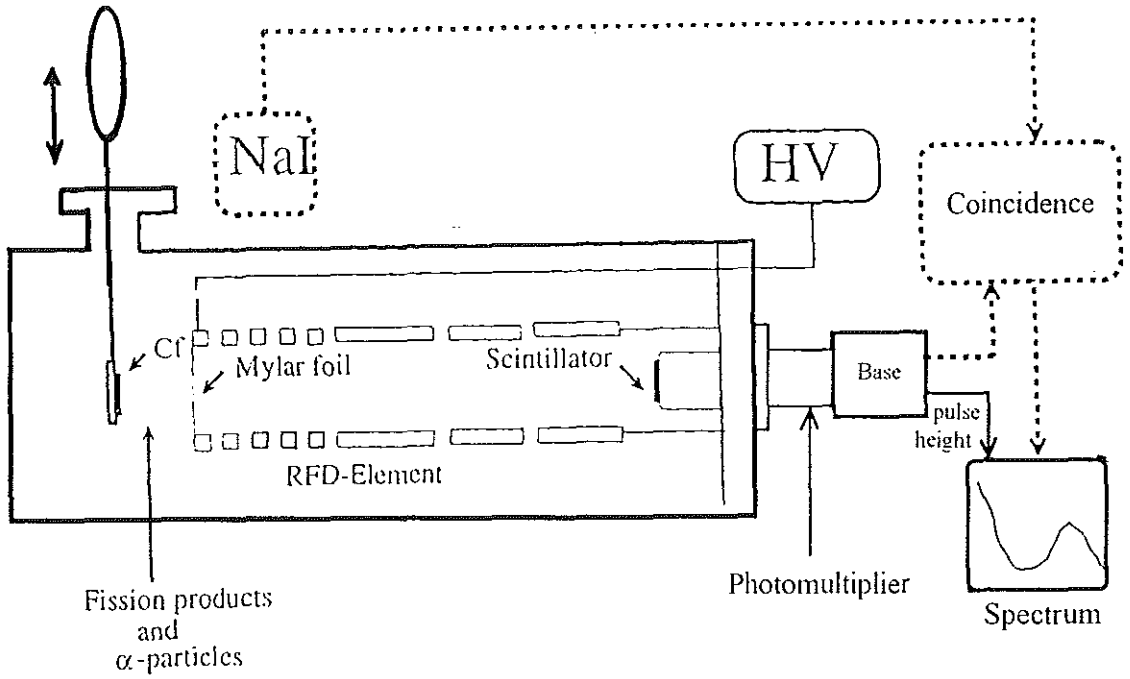

Figure 6: *Schematic view of the experimental setup for the test measurement where the arrangement shown by the dotted lines is used in the coincidence measurements only.*

experimental conditions (the scintillation, the multiplication in the PM and the electronics) are in a good position to run the experiment. This makes observation of the α-particles vital for the intended experiment.

2.1 Measurement of α-particles and Fission products

The main elements of the electronics are shown in fig. 7

The electrons produced in the thin mylar foil by the fission products and α's falling on the scintillator produce light which is collected by the photocathode of

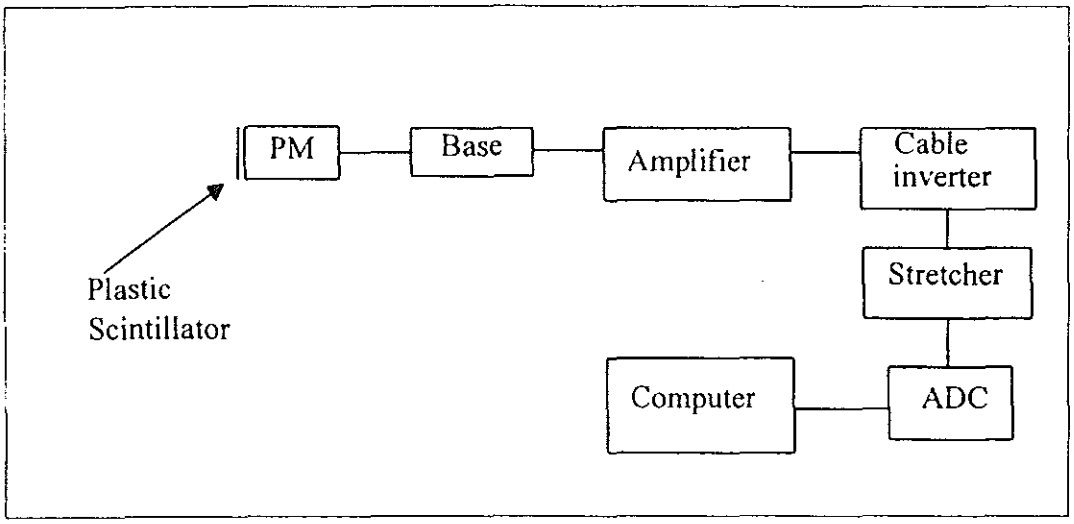

Figure 7: *Scheme of the electronics to measure α-particles and fission products.*

the PM tube. The signals from the photomultiplier are fed to an amplifier by passing through the base. The output signal obtained from the amplifier has a negative amplitude but the stretcher used in the experiment accepts only positive signals. Hence, a cable inverter is included. The stretcher is used to widen the signals because the ADC needs long signals. These analog signals are digitized by the ADC (Analog to Digital Converter) connected to a computer to store the data and to use it for further analysis.

A spectrum of alpha-particles and fission products is shown in fig. 8. It is obtained with an accelerating voltage of -15kV. Measurements were done by varying the accelerating voltage to see the shift of the electron-peak. As expected, when the absolute value of the accelerating voltage is increased, the peak moves to higher channels as shown in fig. 9. On the other hand, the α-peak remains at the same position for different accelerating voltages, because their detection mechanism is

independent of the high voltage applied to the electrodes of the RFD-element.

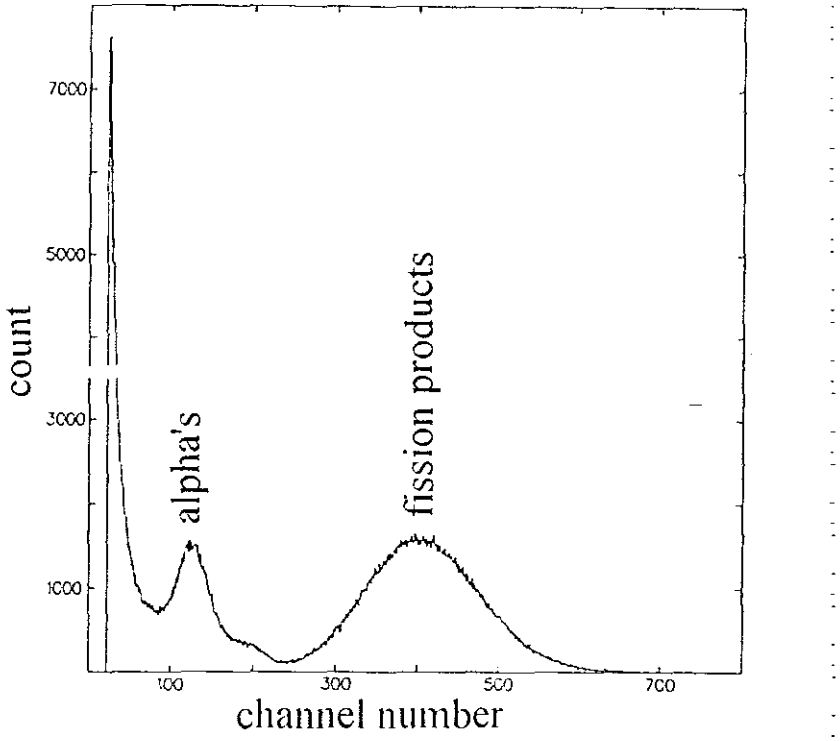

Figure 8: *Spectrum obtained without coincidence with γ-rays and accelerating voltage of $-15kV$.*

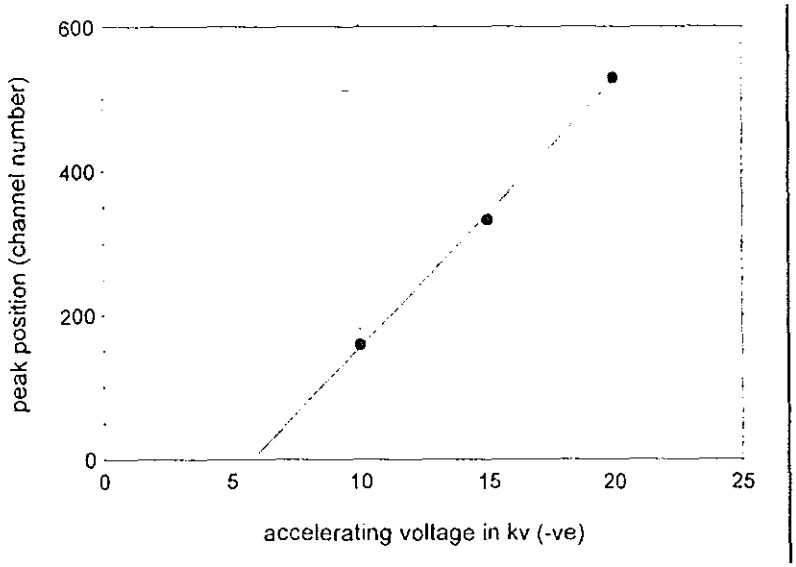

Figure 9: *The electron-peak position as a function of the RFD accelerating voltage.*

2.2 Coincidence Measurements

In every fission process of ^{252}Cf about 8 prompt γ-rays are produced [18], whereas, the α-decay is not accompanied by energetic γ-rays. The main idea of this experiment is to detect the heavy ions created in the fission process in coincidence with the prompt γ-rays and reject the α-particles.

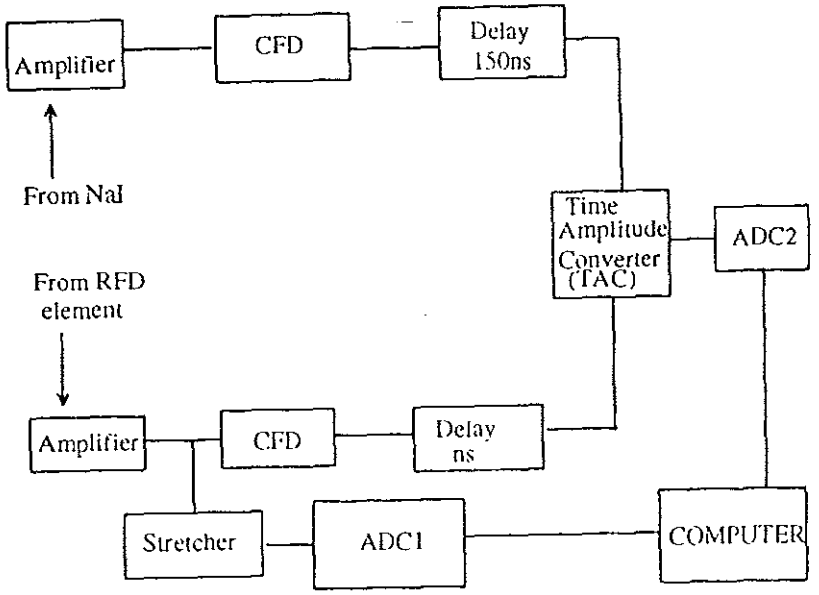

Figure 10: *Scheme of the electronics for γ−fission product coincidence measurements.*

In section 2.1 the setup was arranged to get information only about the pulse height distribution of the particles. As it is seen in fig. 8 there is a large count rate at small channel numbers. Hence, in addition to the pulse height, information about their distribution in time is needed to understand the details of the spectrum. For this purpose the gamma-rays and fission products have to be measured in coincidence

(see again fig. 6).

The details of the electronics arrangement are given in fig. 10. The RFD signal after the amplifier is divided into two signals, one for amplitude information to the ADC1 passing through the stretcher and the other one to a constant fraction discriminator (CFD) for timing purposes.

A NaI detector near by the test chamber is used to detect the prompt γ-rays from the fission process. The signals, after amplification, are supplied to another CFD and delayed by 150 ns.

Both the signals from the RFD and NaI are fed to a Time to Amplitude Converter (TAC) used as coincidence unit (start signal from the RFD and stop signal from the γ-detector). The TAC is connected to ADC2 which is used to digitize the timing signals. The two ADC's are connected to a computer where the data are stored. A two-dimensional plot of the measurement with the accelerating voltage of -20kV is shown on fig. 11. The horizontal axis contains the information about the pulse height (ADC1) and the vertical axis (ADC2) represents the time running from top to bottom.

The fission products are expected to be observed in the scatter plot as sharp in time with a reasonably narrow pulse-height distribution . Events distributed uniformly in time and with low pulse-height are expected as noise signals.

As it is seen in the fig. 11, besides the noise contribution, events are observed in two time windows. The fission products are collected in the first time window

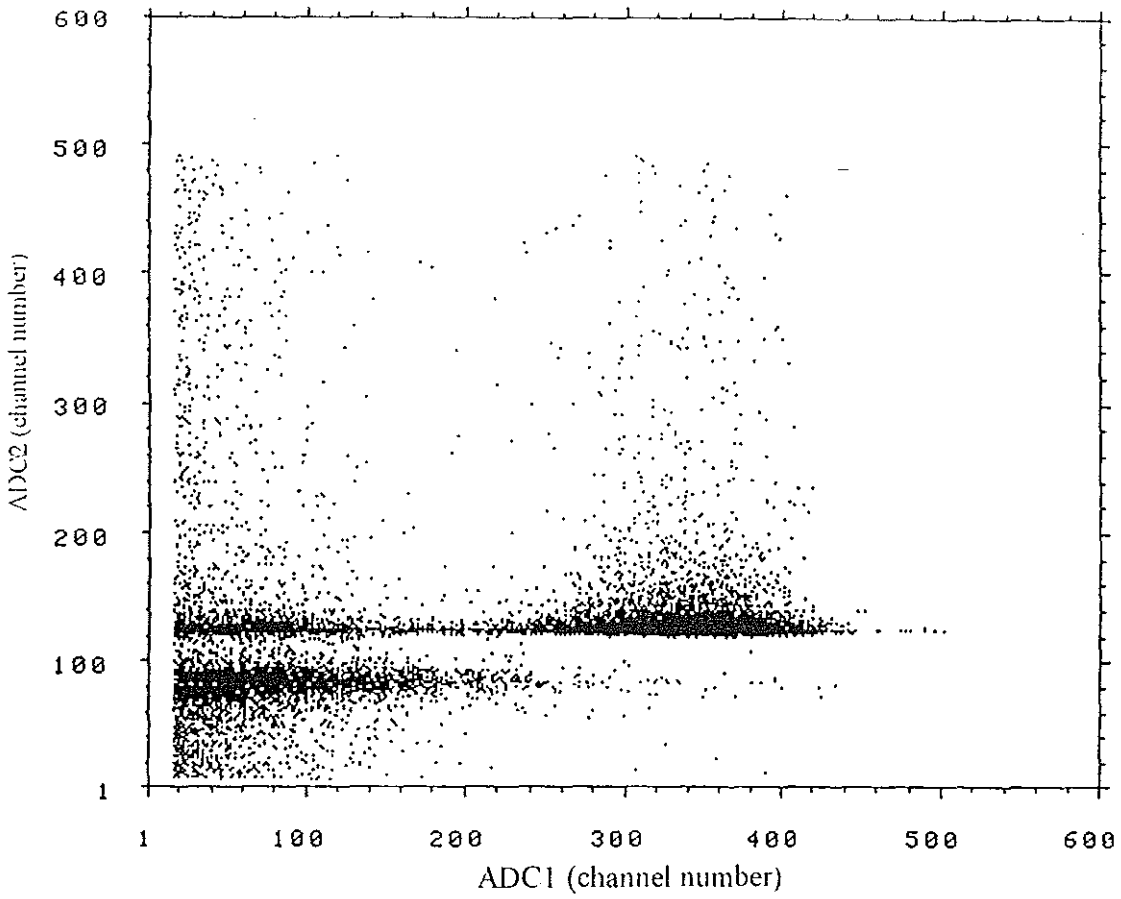

Figure 11: *Two-dimensional spectrum obtained in coincidence measurements with the horizontal and vertical axes representing pulse height and time of flight, respectively (see text).*

near ADC2 channel No. 130 . The origin of events stored in the second time gap is unclear yet. We note also that part of the fission events are shifted to lower energies. Obviously, some fission products create signals with smaller pulse-height indicating some energy loss. The projection of the two-dimensional plot onto the horizontal energy axis (ADC1) is shown in fig. 12(a) and can be compared with the result found without coincidence (fig. 12(b)). The spectra are obtained by adjusting the

accelerating voltage to -15kV. As it can be seen in fig. 12(a), the alpha-particles and large amount of noise events are cleared off. The area under the peak is taken and compared for the two cases (in coincidence and without coincidence). The result shows that 14% of the events registered in the electron peak remain in the coincidence measurement.

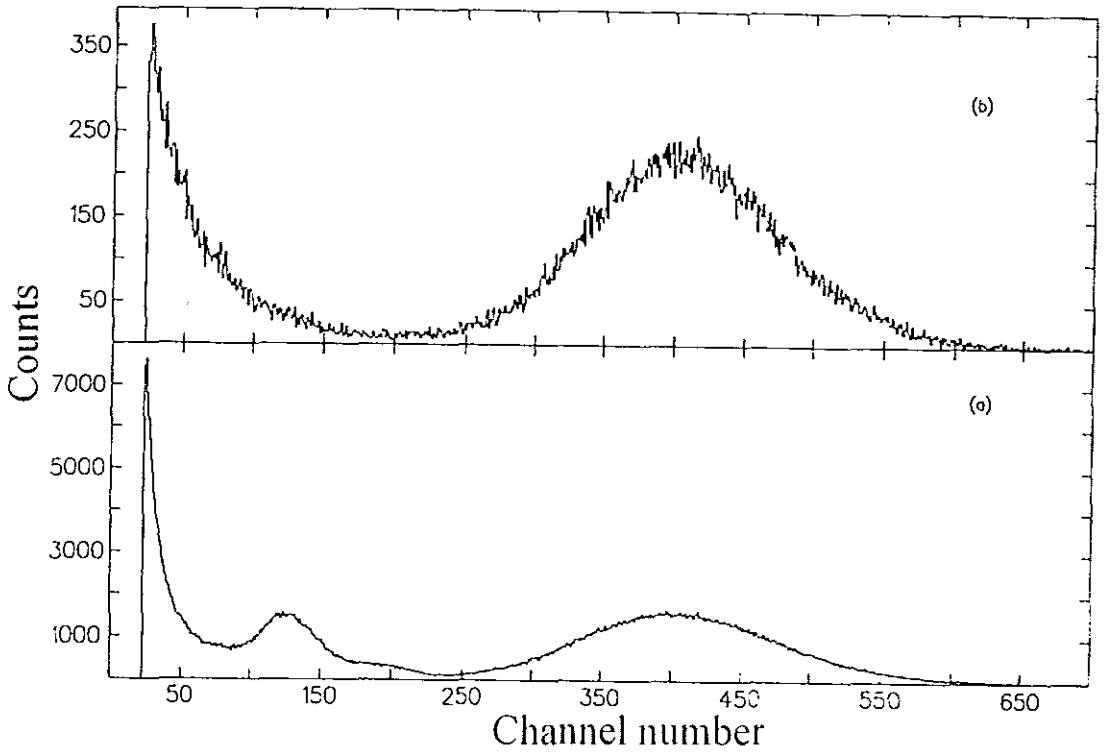

Figure 12: *Spectra found with accelerating voltage $-15kV$ (a) without coincidence (b) γ-fission product coincidence.*

Although the low-energetic background is decreased, there is a considerable amount of coincidence events at low channels. Therefore, additional test measurements were done to check the electronics. The threshold energy of the gamma-rays was changed and for two different threshold energies the following two ratio's were

taken and compared:

a) the ratio of counts in the first time gap with small pulse-height to large pulse-height

b) the ratio of counts in the second time window to the counts of the fission products with high pulse-height.

These ratios are the same with different γ-thresholds leading to the conclusion that the observed noise is not caused by the electronics.

Therefore one has to look for other reason why events are registered at the true time (the first time window) but with small pulse height. One can suspect from fig. 5. where the trajectories of electrons inside the detector element are shown, that it is because of the particles hitting the edge of the foil producing poorly focused electrons. Therefore, it was necessary to check if the fission products hitting the central part and those hitting the edge of the foil create the same pulse height. Experiments were done by covering the edge (an annuls of inner diameter 50mm and outer diameter 60 mm) and central part (diameter of 50 mm) of the mylar foil using a niobium (^{93}Nb) foil of 32 mg/cm^2 thickness. This way we wanted to see if the edge of the RFD-foil is as effective as the center in collecting the electrons. The spectra shown in fig.(13) are obtained by sorting out the events within a time interval according to the channel numbers 120 and 160 of ADC2 (see fig. 11) and projecting them onto the horizontal axis (ADC1). The events in fig. 13, (a), (b) and(c) were collected with the center covered, the edge covered and without any cover, respectively.

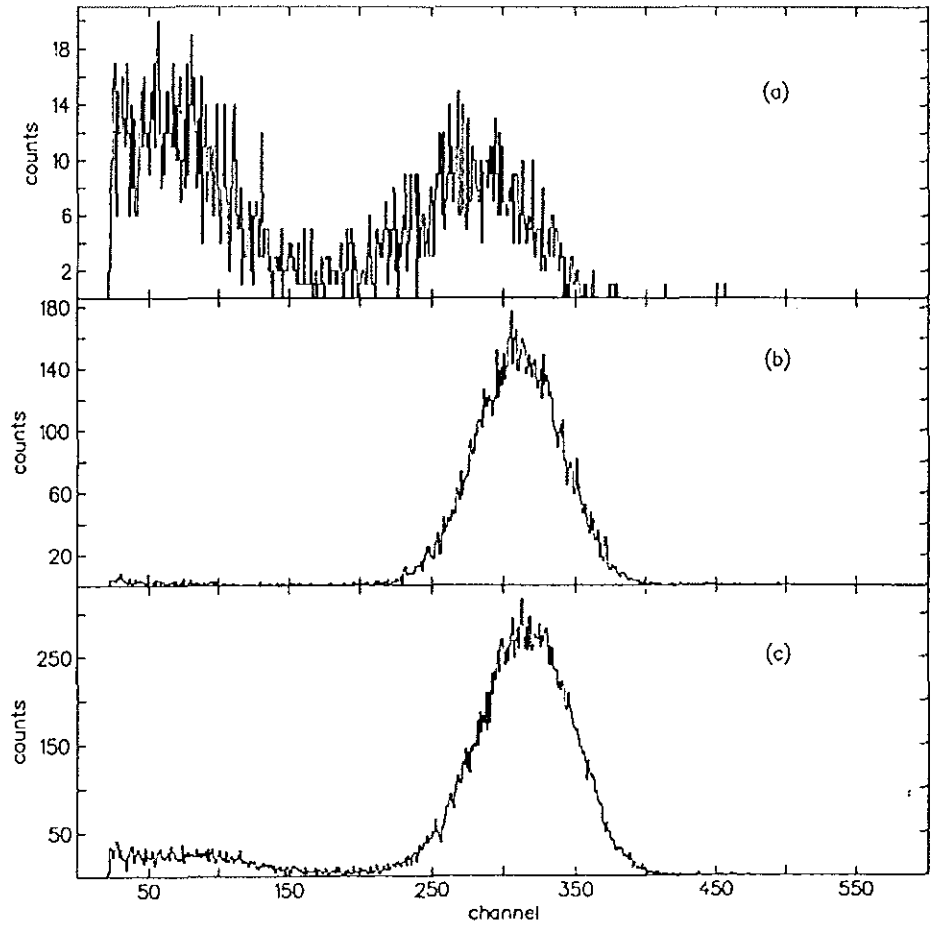

Figure 13: *Projection of the events observed in the first window with (a) the central part of the mylar foil covered (b) the edge covered and (c) without any cover.*

As it can be seen almost all the events registered at the true arrival time of the fission products with small pulse height disappear when the edge of the mylar foil is covered (fig. 13(b)). That means they were created on the edge. The spectrum in fig. 13(a) is analyzed and only 34% of the events were with high pulse-height. Therefore, 66% of the fission products falling on the edge of the foil are registered with small pulse-height and get mixed up with the noise. In the real in-beam experiments the noise events are cut and therefore, 66% of the nuclei hitting the

edge are lost. If one can avoid this loss, then the event rate increases and the detector efficiency increases correspondingly.

In fig. 5, it can be seen that the electrons from the edge fly out of the area covered by the plastic scintillator. A solution was sought for this problem and it was found that instead of mounting the thin foil on the outer edge of the first electrode, it was placed inside at about 4mm from the outer edge. Using the program SIMION [17], the trajectories of electrons for this foil position were calculated and they are presented in fig. 14. The electrons are now well focused on the scintillator, so one can expect an improvement of the detector efficiency.

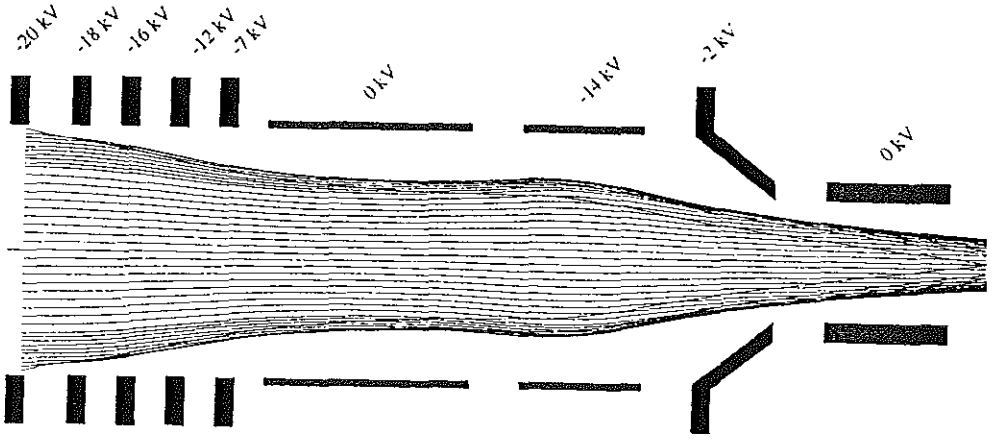

Figure 14: *The trajectories of the electrons with the thin foil placed at 4mm from the outer edge of the first electrode.*

In all test measurements, the events in the second time window seem to be unaffected when the edge or the central part is covered. To exhaust all possibilities data were taken by covering the whole area of the RFD foil. Even in this case the

events are found without any large change in intensity.

Therefore, one has to check if the count rate registered in the second time window depends on the accelerating voltage. For different accelerating voltages, measurements were done under two conditions, namely, covering the whole area of the mylar foil using a niobium(^{93}Nb) foil and keeping it uncovered. As a result the event rate at the same accelerating voltage is found to be almost the same (shown in fig. 15). In both cases the number of counts increases with voltage. This shows that the behaviour of the delayed events is similar to the true events coming from the fission products.

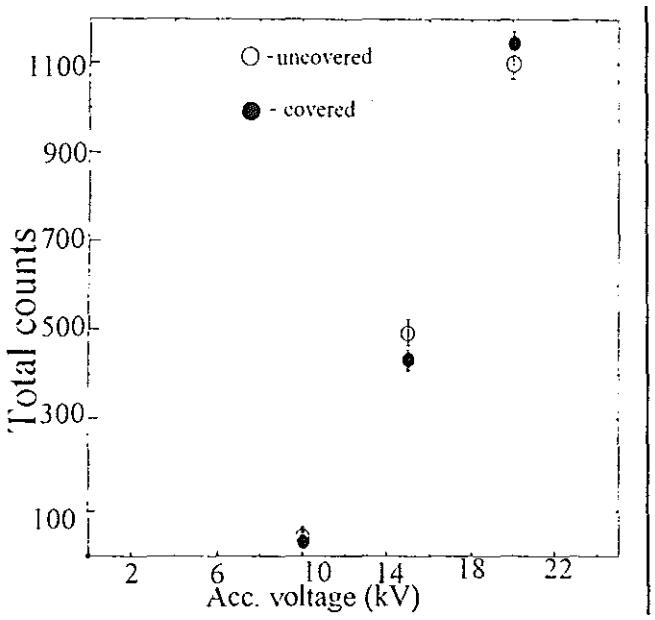

Figure 15: *Total count rate of the delayed events as a function of accelerating voltage with and without covering the mylar foil by a niobium foil.*

The question "where are these particles coming from?" was given attention. One

source could be the wall of the test chamber. A measurement was done by inserting a diaphragm (hole of diameter 30mm) between the ^{252}Cf source and mylar foil. Data were taken for two positions of the diaphragm, 20mm and 9mm from the source, respectively. In the first case the wall close to the RFD-element cannot be reached by the source particles.

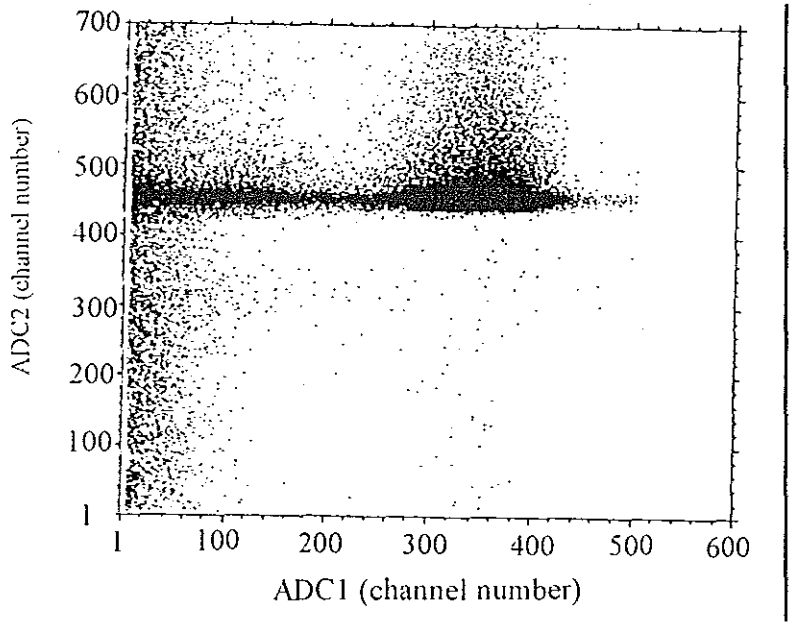

Figure 16: *Scatter plot obtained by inserting a diaphragm between the source and RFD foil.*

The scatter plot shown in fig. 16 is obtained with the first arrangement. The unknown events arriving later than the fission products disappeared. But, when the diaphragm is positioned at 9mm from the source, enabling fission fragments to irradiate the wall, those delayed events appeared again. Therefore, one can conclude that the fission products interact with the wall and some kind of positive charges may be produced which will be accelerated towards the RFD-element. These charges

may hit one of the RFD-electrodes and production of electrons may follow. Then, the electrons will be focused on the plastic scintillator.

Hence, these delayed events are related only to the particular arrangement of our test setup and they do not create any problem for the in-beam experiments. As the main result of the test experiments, one can conclude that the source of the low RFD efficiency (below the theoretical estimation) is caused by the position of the thin mylar foil. The electrons produced on the edge of the foil are not focused on the scintillator. The solution of this problem is to change the position to a distance of 4mm from the outer edge of the first electrode of the RFD-element. The electrons from the whole area of the mylar foil are now collected (shown in fig. 14). Using this new geometry, in in-beam experiments, nuclei hitting the edge will not be lost and therefore an increase in efficiency.

3 Detector Using Backward Emitted Electrons

3.1 Introduction

When a proton, an alpha-particle or another heavy ion moves through matter, it ionizes or excites the atoms to which it comes sufficiently close. This change of the atomic state are caused by the Coulomb force, which can transfer kinetic energy/momentum to an electron as the particle moves swiftly by [21, 22]. The energy transferred to the electron represents a loss of kinetic energy of the bombarding particle, which will slow down and eventually stop. This can result in the emission of electrons, especially from the surface of the material irradiated. This phenomenon was first observed under electron beam impact and is referred to as secondary electron emission (SEE). SEE provides information on the processes occurring during the passage of charged particles through matter and on the escape mechanism of electrons from solids. A good understanding of SEE is of general importance for the development of heavy-ion detectors.

SEE is observed in the forward and backward direction provided that the target is sufficiently thin. The foil is called thin in this context, if $\Delta E_p \ll E_p$, where E_p is the energy of the projectile and ΔE_p is the energy it loses while penetrating the foil [19, 23].

Usually, the total electron yield γ_T is defined as the number of electrons per impinging primary particle emitted in the whole solid angle. The backward secondary electron yield (γ_B) can be defined as the number of electrons emitted in the back-

ward direction per primary particles and the same is true for the forward secondary electron yield (γ_F).

In almost all studies of SEE following ion penetration into thin foils for a given projectile velocity, γ_F is always higher than γ_B for all projectile/ target combinations, i.e SEE in the forward direction dominates [18, 23, 24]. From this point of view, it is understandable to use the Recoil Filter Detector(RFD) collecting the electrons emitted in forward direction.

However, there are disadvantages when using RFD. The production of thin foils is in general a rather difficult task avoidable if one uses the electrons emitted in the backward direction. For practical reasons the foils cannot be made thinner than about 50Å. To fulfill the condition $\Delta E_p \ll E_p$ the ion velocity must be of the order of $v_p^2 = E_p/M_p > 30keV/u$. Slow particles may not be detected even under the most favorable conditions (extremely thin target foil). This is because electron emission in the forward direction is from the exit surface and the low energy ions may not reach the exit surface.

For the new detector principle, the electrons in the backward direction are from the entrance surface, and the ions do not have to pass through the foil. The other shortcoming in using RFD is the dead space between the detector elements, only 2/3 of the total area(between the angles 2.7^0 and 12.1^0) is active (see ref.[10, 14]).

Therefore, the development of a detector device using the backward emitted electrons is desirable to measure low-energetic nuclei produced in in-beam heavy-ion reactions.

3.2 The Designing Process

The designing is done under the assumption that there is a beam of particles colliding with a target located at a distance of about 70cm from the point where the electron emitting material should be placed. The detector is intended to measure recoiling nuclei emerging in a narrow cone between 3^0 and 15^0 in the beam direction. As in the RFD case the central part (below 3^0) must be left open, letting the direct beam particles pass through.

The aim is to design a detector for heavy particles whose geometry looks like as given in fig.(17).

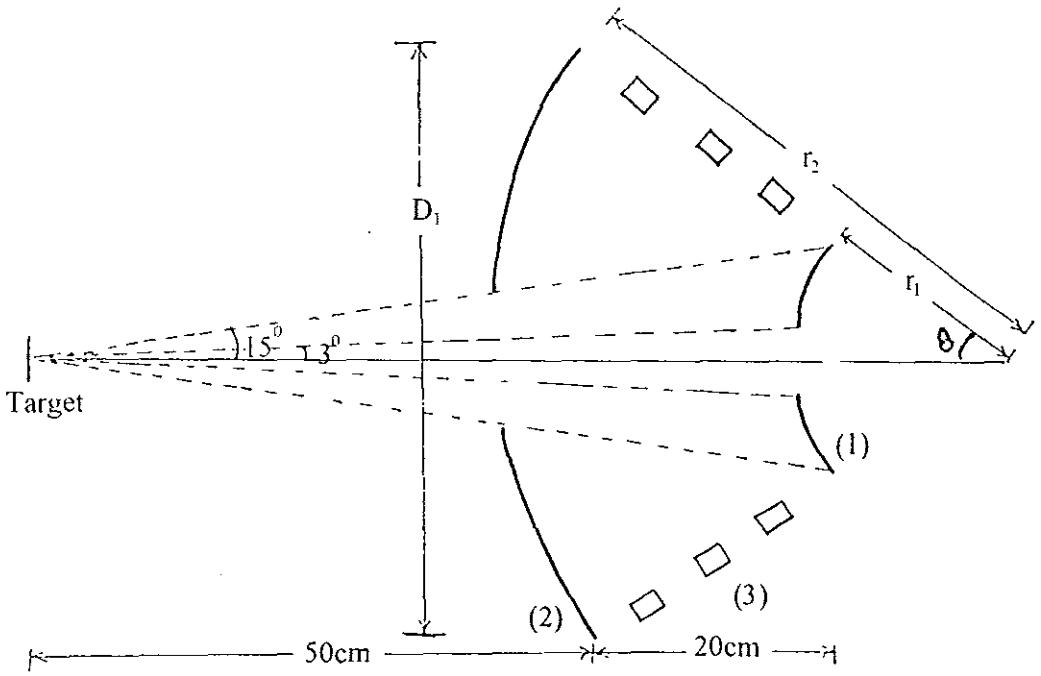

Figure 17: *Sketch of the newly planned heavy- particle detector which uses the backward emitted electrons.*

The surface indicated by (1) is an electrode which will be maintained at negative high voltage of about -20kV. Particles coming out of the target between 3^0 and 15^0 strike the surface (1) and electrons will be emitted. Because of the negative potential supplied to (1), the electrons will be accelerated to the other surface denoted by (2) (zero potential). Surface (2) will be covered with a scintillator subdivided into small parts. The structure allows to identify the place where the electrons are created on the electron emitting electrode (1). This determines the recoil angle and the distance from the target,and by measuring the time of flight of the heavy ions. Doppler correction can be carried out. The electrodes (3) kept at different potentials will be placed in between the two surfaces to shape the trajectories of the electrons.

The best guideline for the electron optics is to assume two concentric spheres supplied with a corresponding potential difference. An electron created on the surface of the inner sphere will be accelerated radially outward by the potential difference. So, the idea is to put an electron emitting material at the position of the inner sphere and a scintillator at the position of the outer sphere. For such an arrangement the potential between the two spheres is governed by the equation

$$V = \frac{A}{r} - B \tag{4}$$

where A and B are constants and r is the radial distance.

When the boundary conditions are applied i.e when the inner sphere is set to -20kV and the outer is taken to be grounded, the following relations are obtained

$$\frac{A}{r_1} + B = -20 \tag{5}$$

$$\frac{A}{r_2} + B = 0 \tag{6}$$

where r_1 and r_2 are the radii of the inner and outer spheres, respectively. The solutions for the constants A and B are

$$A = -20\frac{r_1 r_2}{r_2 - r_1} \qquad inkV\,cm \tag{7}$$

$$B = 20\frac{r_1}{r_2 - r_1} \qquad inkV \tag{8}$$

Of course, the detector cannot be made of two complete concentric spheres. There has to be an opening on the outer sphere to let the reaction products in and hit the inner one. Since the particles to be detected are coming out of the target in a narrow cone, the opening angle is set to be 15^0. For the direct beam a hole in the inner sphere must be made (opening angle 3^0). For practical reasons the distance D_1 indicated in fig. 17 is needed to be about 50 cm, which gives

$$r_2 \sin\theta = 25cm \tag{9}$$

If the length of the detector will be about 20cm, then

$$r_2 \cos\theta - r_1 \cos\theta = 20cm \tag{10}$$

On the other hand, the −20kV-electrode should be at about 70cm from the target , therefore

$$r_1 \sin\theta = 70 \tan 15^0 cm \tag{11}$$

Subtracting equ. (11) from (9) and dividing by equ. (10) gives

$$tan\theta = 0.312 \quad i.e \quad \theta = 17.34^0 \tag{12}$$

Substituting this value in equs. (9) and (11) one obtains the radii of the two concentric spheres

$$r_1 = 62.93\, cm \qquad \text{and} \qquad r_2 = 83.88\, cm$$

With these values of r_1 and r_2 the constants A and B are found to be

$$A = -5039.2 \text{ kVcm} \qquad \text{and} \qquad B = 60.1 \text{ kV}$$

Therefore, the potential between the two concentric spheres as a function of the radial distance is given by

$$V = \frac{-5039.2kV\,cm}{r} + 60.1kV \tag{13}$$

where r is the radial distance in cm.

Relation 13 is used to place electrodes in between the two concentric spheres. The program SIMION [17] is then used to calculate the electron trajectories and equipotential lines inside the detector. In the beginning, the electrons are observed flying radially outward as shown in fig. 18. Some of them move out through the hole because the parameters are fixed by using equ.(13) obtained for concentric spheres. Therefore, those electrons which do not reach the outer sphere should be bent to hit the outer sphere. For this reason the −20kV-electrode is made of conical form

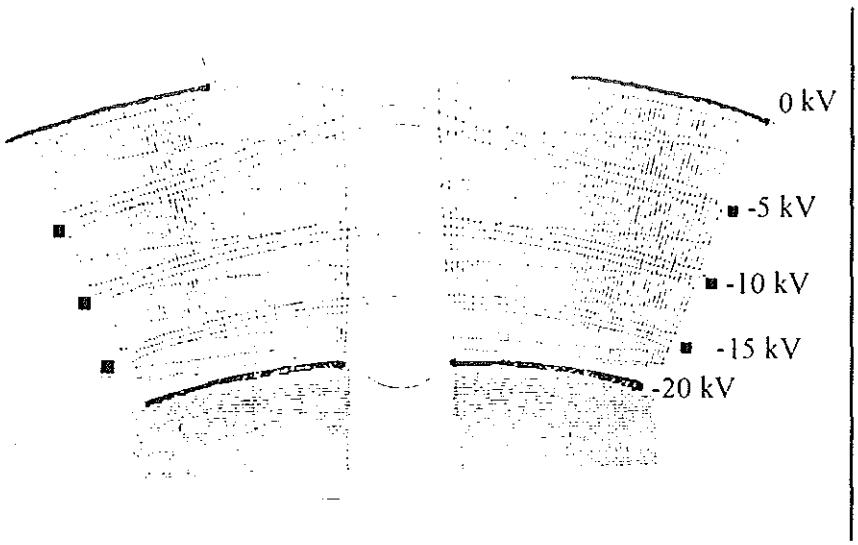

Figure 18: *Cross section of the two concentric spheres and electrodes. With the potentials indicated. the trajectories of the electrons are obtained . The holes in the inner and outer spheres correspond to the opening angles of* 3^0 *and* 15^0*. respectively.*

with half angle 60^0 keeping in mind the 3^0 opening angle to be there. Since the surface of the outer sphere will be covered by a scintillator. technically it is easier to make this part conical rather than spherical. For better collection of the electrons. the half angle of the cone should be 55^0. In addition to these two cones. electrodes of different potentials are placed to shape the electron trajectories. This correction is necessary especially for electrons from the outer edge of the electron-emitting electrode. Another electrode is placed on the inner edge of the -20kV-electrode to bend the electrons from this edge and force them to reach the 0kV-electrode.

As it can be seen from fig. 19. some electrons do not reach the scintillator. This loss must be accepted because if they are bent to some part of the detector. the accuracy of the Doppler-shift correction would inevitably decrease.

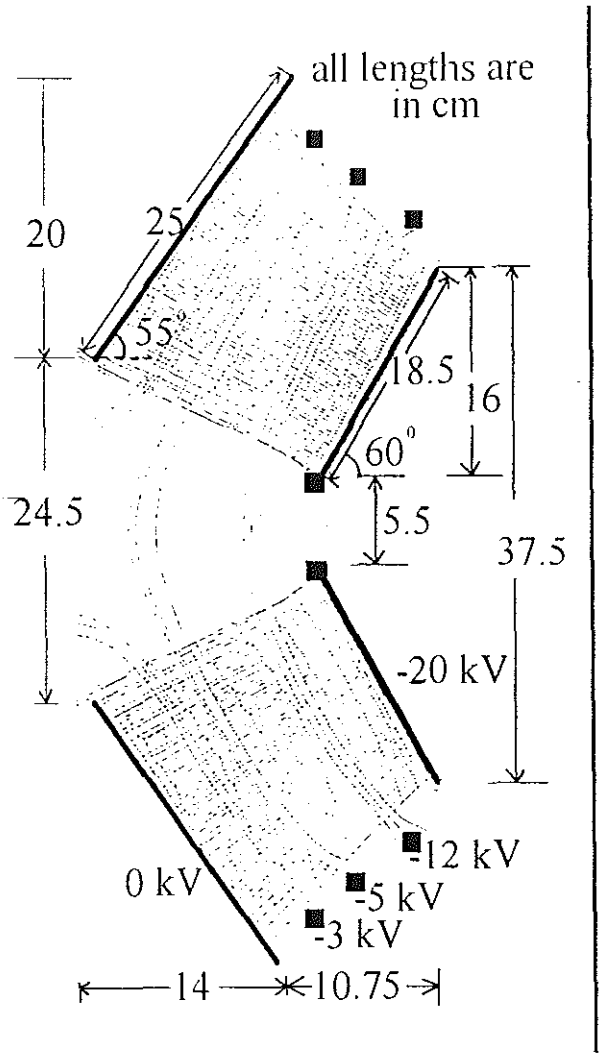

Figure 19: *Cross sectional view of the design of a detector which uses backward emitted electrons.*

For the purpose of the Doppler-shift correction, the scintillator must be subdivided into small parts. The Doppler-shift of the γ-rays emitted from recoiling nuclei in linear approximation is given by [25]

$$\Delta E_\gamma = E_\gamma \beta_r \cos\theta_o \tag{14}$$

where E_γ is the energy of the gamma-ray, β_r is the recoil speed divided by speed of light and θ_o is the recoil angle.

In order to determine the velocity vector of the recoiling nuclei, one must know the distance it has traveled, the time of flight and the scattering angle. These quantities cannot be measured exactly. The uncertainty caused by measuring these quantities is wanted to be kept below 1keV. From equ.(14), the following relation can be derived

$$\Delta(\Delta E_\gamma) = E_\gamma cos\theta_\gamma \Delta\beta_r - E_\gamma \beta_r sin\theta_\gamma \Delta\theta_\gamma \tag{15}$$

Here it can be seen that the uncertainty in θ_γ is not important for a Ge detector placed at 0^0, which gives

$$\Delta(\Delta E_\gamma)/E_\gamma = \Delta\beta_r \tag{16}$$

If the gamma-energy is around 1MeV and $\beta_r \leq 0.03$, then for the energy uncertainty of about 1keV one obtains

$$\Delta\beta_r \approx 0.001 \tag{17}$$

and

$$\Delta\beta_r/\beta_r = \Delta l/l \approx 1/30 \tag{18}$$

For the other extreme case, if the detector is placed at 90^0, the uncertainty in θ_γ becomes important and with the above assumptions of $E_\gamma \approx 1MeV$, $\beta_r \leq 0.03$ the angular uncertainty is limited to

$$\Delta\theta_s \approx 1/30 \approx 2^0 \tag{19}$$

Since there is an angular uncertainty of $6^0 - 8^0$ due to the size of the germanium detectors, even a somewhat larger angular uncertainty of the order of 3^0 can be tolerated.

The idea is to subdivide the scintillator area into small hexagons whose size can be determined using the uncertainties in length (equ.(18)) and angle (equ.(19)). Accordingly, it is found that 90 subdivisions can be made. In contrast to the RFD there is no empty space between the small detector areas.

The division of the scintillator plane helps to do the Doppler-shift correction in the following way. Each small area on the scintillator has its opposite on the electron emitting electrode. In principle, all electrons emitted from every small part should fall on the corresponding area of the scintillator. If one knows from which part of the electrode the electrons are emitted, then the recoil angle and the distance it has traveled is known. But, it may happen that, electrons from different parts of the electrode may overlap on one scintillator division. This means two different heavy ions with different recoil angle emit electrons from two different parts but these may fall on one scintillator division and they may be treated as if they were emitted from one part and by nuclei with the same recoil angle. This creates a problem for the correction. The only way to avoid this problem is not to detect those overlapping electrons. This can be done by defining the parts where these electrons are coming from as dead.

The scintillator area on which overlap is observed depends on the emission energy of electrons. It is known that most of the electrons are emitted with energy less than 10 eV [18]. For this, the electron-trajectories are calculated (using the program SIMION [17]) by varying the energy. Electrons emitted from one point with a certain energy and with different emission angle hit at different points of the scintillator. The calculation is done for different emission angles (from -90^0 to 90^0 measured from the normal of the surface). The electrons are distributed in a certain range where the width of this range depends on the energy. The width as obtained from the calculation is plotted in fig. 20 as a function of energy. As it is seen the width is increasing with energy. One can expect from a rough calculation that the width is proportional to the square root of the energy.

The subdivision of the scintillator is planned to have a size of 4cm. and the width obtained for 10eV emission energy is about 1.5cm which is comparable to the size of the subdivision. But the width is as small as 0.6cm for 2eV. This shows that it is strongly dependent on the emission energy. Although it is known that most electrons are emitted with energies less than 10eV, the detectors used for this purpose are not efficient enough for energies smaller than 10eV [9]. Therefore, it would be essential to know the energies of the emitted electrons with higher accuracy.

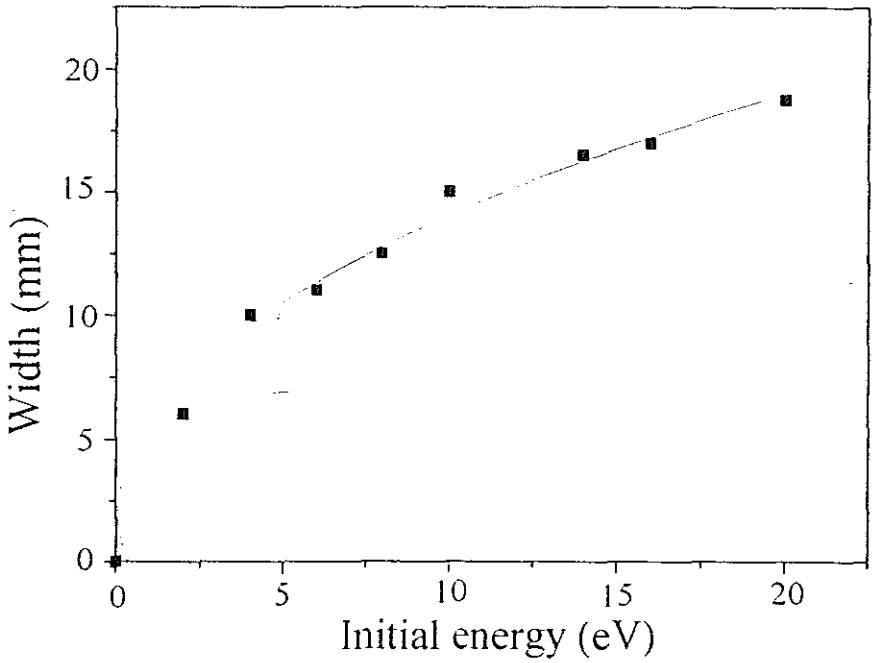

Figure 20: *The width of the electrons' distribution at the scintillator position as a function of their emission energy.*

3.3 Test Measurements

Experiments were done in order to see if the idea of using backward emitted electrons is promising.

The electronics was the same as the one used for coincidence measurements using the RFD element (see fig.(10)). The difference is the way the element used was placed inside the test chamber. Accordingly, the position of the source was also changed.

For a test experiment the element used was a very simple one. It consists of two electrodes of which one is supplied with negative high voltage and the other

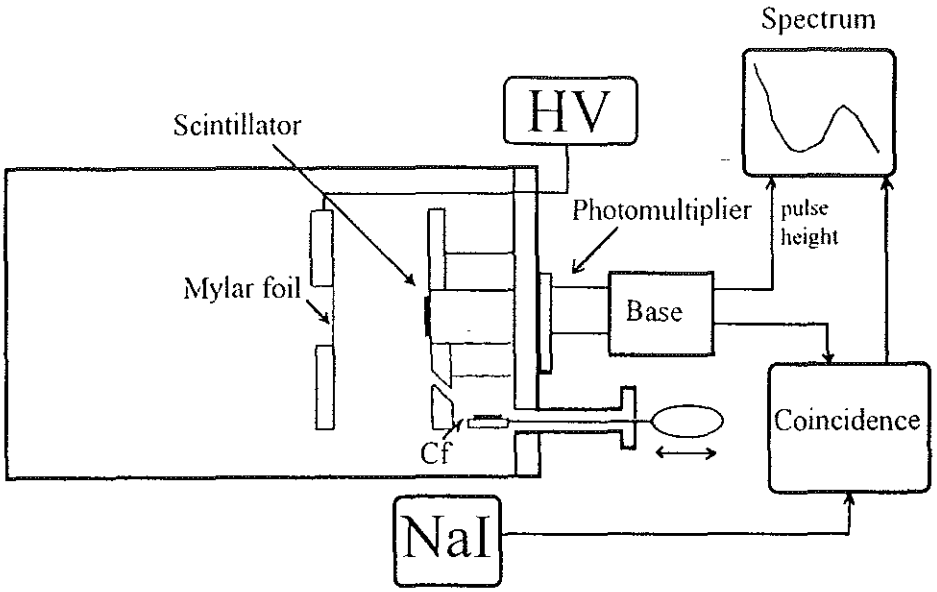

Figure 21: *The experimental setup for observing the backward emitted electrons.*

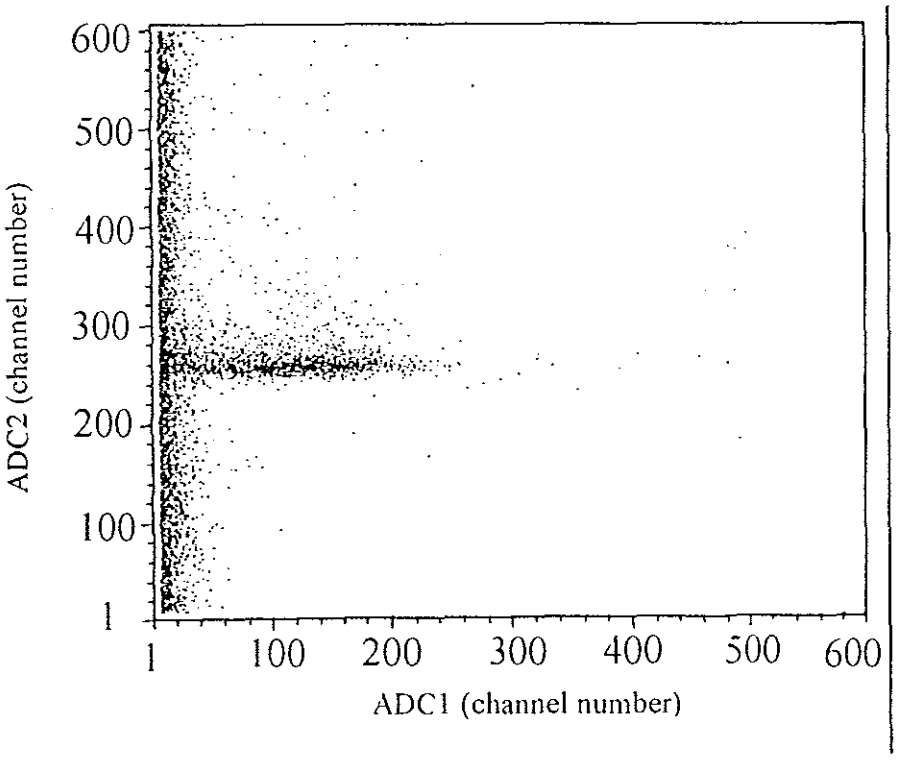

Figure 22: *Two dimensional plot (time versus pulse height) obtained with backward accelerating element used in place of the RFD element.*

is grounded. There is a thin foil of thickness 0.5μm and diameter of 4cm mounted on the electrode with high potential. A hole on the other electrode allows the heavy fission products to pass through and hit the foil. Electrons emitted in the backward direction will be accelerated (without any focusing) towards the scintillator counter, and the signals are treated as described in section 2.1. The experimental arrangement is shown in the fig. 21.

The event distribution obtained is shown in fig.(22). One can see that one group of events arrive within a very small time interval around channel number 260. These signals obviously are created by fission fragments. The randomly time-distributed signals at small pulse height constitute noise events. Their number is much larger (compared to the true events) than in the case of the RFD-element (see fig. 11). This fact is a conssequence of the small yield of backward emitted electrons.

4 Conclusions

The work is divided in two parts, the test experiment done with the existing RFD-element and the designing of a detector which uses electrons emitted in the backward direction.

The first part of the work was aimed at finding the reason for the low efficiency of the Recoil Filter Detector and giving a solution to increase the efficiency. It was found that the electrons emitted from the edge of the thin mylar foil are not well focused on the plastic scintillator. This focusing property of the element was found to be sensitive to the position of the mylar foil. The optimum condition was found to be moving it by 4 mm from the outer edge of the first electrode and the efficiency should be larger, because the large electron loss is now avoided. A real in-beam experiment must be carried out to check this finding.

In the second part, design studies of a heavy-particle detector which uses backward emitted electrons was made. This detector turned out to be a good alternative, and in some cases, especially for low-energy recoiling nuclei it may replace the existing RFD. The advantages over the Recoil Filter Detector are:

- It does not use thin foils which are difficult to prepare because the electrons are emitted from the entrance surface of the foil while for the RFD they are emitted mainly from the exit surface.

- Backward emission of electrons has the advantage to move the energy threshold of ions to lower energies.

Its active detector area can be made larger than for the RFD. Empty space between the detector elements does not appear.

Most electrons emitted backwards have energies lower than about 10eV. However, the correct energy distribution is not well known. Therefore, further experimental tests are necessary to investigate the focusing properties of the new detector crucial for Doppler shift corrections. Only then this trigger detector can be used in advanced in-beam experiments with other detector arrays like OSIRIS.

References

[1] J. M. Blatt and V. F. Weisskopf, Theoretical Nuclear Physics, John Wiley & Sons, New York, 1966.

[2] H. G. Clerc *et al.*, Nucl. Phys. A419 (1984)571.

[3] C. Ngo, In "Heavy Ion Fusion Reactions", Proc. of the Tsukuba International Symposium, World Scientific, Singapore, 1984.

[4] U. Mosel, In "Dynamics of Heavy-Ion Collisions", Proc of the 3rd Adriatic Europhysics Study Conf, North-Holland, Amsterdam, 1981.

[5] J. O. Newton, In "Progress in Nuclear Physics" (D. M. Brink and J. H. Mulvey ed.) Vol. XI, pp. 53–144, Pergamon, Oxford, 1969.

[6] S. Cohen *et al.*, In "Proc. Conf. Reactions between Complex Nuclei", Asilamor, California, pp 325, Univ. of California Press, Berkeley, 1963.

[7] R. Beringer, and W. J. Knox, Phys. Rev. 121 (1961)1195.

[8] C. Ngo *et al.*, Nucl. Phys. A400 (1983)259c.

[9] P. Spolaore *et al.*, Nucl. Instr. and Meth. A238 (1985)381.

[10] J. Heese *et al.*, Phys. Lett. B302 (1993)390.

[11] J. Heese *et al.*, "Development of a new recoil detector for γ-detector arrays": private communication.

[12] K. Spohr *et al.*, Gamma spectroscopy with the recoil filter detector. Recent results and perspectives: private communication.

[13] K. Spohr *et al.*, Spectroscopy with large γ-arrays in coincidence with a RFD: private communication.

[14] G. F. Knoll, Radiation Detection and Measurement, John Wiley & Sons, New York, 1989.

[15] K. Spohr, Spektroskopie der schweren neutronenarmen Kerne ^{189}Pb und ^{199}At, sowie des Kerns ^{57}Ni und Entwicklung eines Detektors fuer Verdampfungsrest kerne; Diss. Universitaet Bonn, 1996.

[16] K. Spohr *et al.*, In "Annual Report of HMI-Berlin", Berlin, pp 108 & 114, Hahn-Meitner-Institut Berlin , 1994.

[17] D. A. Dahl, The SIMION PC/Ps2 Users Manual, Idaho Nat. Eng. Lab., Idaho Inc., April 1988.

[18] Rothard H. *et al.*, Kinetic Electron Emission from Ion Penetration of Thin Foils in Relation to the Pre-equilibrium of Charge Distributions, Particle Induced Electron Emission II, Springer Tracts in Modern Physics, Vol 123, 97–147, Berlin–Heidelberg, 1992.

[19] R. B. Firestone and E. Browne, Table of Radioactive Isotopes, John Wiley & Sons, New York, 1986.

[20] R. D. Evans, The Atomic Nucleus, McGraw-Hill, New York, 1955.

[21] R. M. Singru, Introduction to Experimental Nuclear Physics, Wiley Eastern pr.Ltd, New Delhi, 1974.

[22] H.G. Clerc *et al.*, Nucl. Instr. and Meth. 113 (1973)325.

[23] J. Schader *et al.*, Nucl. Instr. and Meth. 151 (1978)563.

[24] H. P. Garnir *et al.*, Nucl. Instr. and Meth. 202 (1982)187.

[25] H. Morinaga and T. Yamazaki, In-beam Gamma-ray Spectroscopy, North Holland, Amsterdam, 1976.

DECLARATION

I, the undersigned, declare that the thesis is my original work, has not been presented for a degree in any other university and that all sources of material used for the thesis have been duly acknowledged.

Name: Haile Gebremariam

Signature: _____

Physics Department, A. A. U.

June, 1996

This thesis has been submitted for examination with my approval as university advisor.

Name: Siegfried Tesch

Signature: _____